Atmos. Chem. Phys. Discuss., 2, 2259–2296, 2002
www.atmos-chem-phys.org/acpd/2/2259/

Atmospheric Chemistry and Physics Discussions

Partitioning of reactive nitrogen (NO_y) and dependence on meteorological conditions in the lower free troposphere

C. Zellweger[1], J. Forrer[1,3], P. Hofer[1], S. Nyeki[2,4], B. Schwarzenbach[1], E. Weingartner[2], M. Ammann[2], and U. Baltensperger[2]

[1]EMPA, CH-8600 Dübendorf, Switzerland
[2]Paul Scherrer Institute, CH-5232 Villigen PSI, Switzerland
[3]Now at University of Zürich, CH-8057 Zürich, Switzerland
[4]Institute for Environmental Research, University of Essex, Colchester, UK

Received: 11 October 2002 – Accepted: 12 November 2002 – Published: 2 December 2002

Correspondence to: C. Zellweger (christoph.zellweger@empa.ch)

Abstract

Results of continuous nitrogen oxide (NO), nitrogen dioxide (NO_2), peroxyacetyl nitrate (PAN) and total reactive nitrogen (NO_y) measurements along with seasonal field campaigns of nitric acid (HNO_3) and particulate nitrate (NO_3^-) measurements are presented for a two-year period at the high-alpine research station Jungfraujoch (JFJ), 3580 m asl. The NO_y mixing ratio and partitioning is shown to strongly depend on meteorological conditions. Knowledge of these meteorological transport processes allows discrimination between undisturbed (i.e. clean) and disturbed (i.e. influenced by regional pollution sources) free tropospheric (FT) conditions at the JFJ. Median NO_y concentrations during undisturbed FT periods ranged from 350 pptv (winter, December to February) to 581 pptv (spring, March to April). PAN was found to be the dominant NO_y species during spring and summer, whereas NO_2 was most abundant during autumn and winter. Particulate nitrate was found to contribute significantly to total NO_y during thermally induced vertical transport. Föhn events, synoptical lifting (e.g. fronts) and thermally induced vertical transport resulted in mixing ratios up to 10 times higher at the JFJ compared to undisturbed FT conditions. Furthermore this meteorological variability of the NO_y concentration and partitioning often dominated the seasonal variability. As a consequence the use of filters at the JFJ (and other mountainous sites) is crucial for the interpretation of data from such measurement sites. This study presents a further development of meteorological filters for the high-alpine site Jungfraujoch, which could be adapted to other mountainous measurement sites.

1. Introduction

Reactive nitrogen compounds play a central role in the chemistry of the troposphere. Nitrogen oxides (NO_x = NO + NO_2) are the limiting precursors for O_3 production throughout most of the troposphere, and also directly influence the abundance of the hydroxyl radical concentration in the troposphere (e.g. Crutzen, 1979; Roberts, 1995).

ACPD

2, 2259–2296, 2002

Emissions of reactive nitrogen occur primarily as NO, followed by oxidation to NO_2. Reactive nitrogen, abbreviated NO_y, is defined as the sum of NO_x and its atmospheric oxidation products, abbreviated NO_z. NO_2, peroxyacetyl nitrate (PAN), nitric acid (HNO_3) and particulate nitrate (NO_3^-) are considered to be the most abundant NO_y compounds in the troposphere, while their relative abundance varies significantly. For instance, NO_2 is often dominant close to sources; PAN tends to be most abundant in regionally polluted air masses where there is more active organic photochemistry; and inorganic nitrates are most abundant in the more remote areas of the troposphere. However, there is significant uncertainty in the levels and speciation of NO_y in the non-urban troposphere due to a lack of measurements (Carroll and Thompson, 1995).

In the present study, we present a two-year time series of total and speciated NO_y from the high Alpine Research Station Jungfraujoch (JFJ), Switzerland. This is the first data series on nitrogen oxides levels in the free troposphere over Central Europe. Ongoing measurements at the JFJ of NO, NO_2 (since June 1991) and total NO_y (since March 1997) were accompanied by PAN measurements (March 1997 to April 1998) and seasonal measurement campaigns of particulate nitrate and HNO_3 (between July 1997 and April 1998). In contrast to previously published work (Zellweger et al., 2000) the focus of this paper is on the seasonality of NO_y and its constituents in the undisturbed troposphere over Central Europe. Further attention was also given to the identification of meteorological transport processes that occasionally cause pollution episodes at the JFJ.

The JFJ is one of the 16 measurement sites of the Swiss National Air Pollution Monitoring Network (NABEL). Furthermore, the JFJ high-alpine station has been the site of an aerosol program since 1988 (Baltensperger et al., 1997; Lugauer et al., 1998; Nyeki et al., 1998). Due to the importance of monitoring long-term trends of gaseous and aerosol parameters in the remote troposphere, the JFJ station has been incorporated into the Global Atmosphere Watch (GAW) program of the World Meteorological Organization (WMO). The JFJ is also part of the combined European GAW virtual baseline station, additionally comprising the Zugspitze (2962 m, Germany) and Sonnblick

ACPD
2, 2259–2296, 2002

(3106 m, Austria) high-alpine stations.

Although air-quality monitoring networks provide observations of the spatial and temporal variation of trace gases, they usually provide no information on chemistry above ground and higher. Aircraft observations have shown that surface and upper air chemistry are frequently decoupled (Berkowitz et al., 1998). As a consequence, surface measurements are in general only representative of measurements near the ground. In contrast, mountainous stations are often decoupled from the planetary boundary layer and measurements are therefore representative of a larger region. Nevertheless, it is also important to develop methods to detect periods of local or regional pollution at mountainous stations. The influence of different meteorological processes on the NO_y mixing ratio at the JFJ is specifically considered in this paper in order to better quantify disturbed and undisturbed free tropospheric (FT) conditions, and hence aid in the interpretation of long-term measurements.

2. Experimental

Total NO_y measurements began in March 1997 at the JFJ. While the measurements of NO, NO_2 started in June 1991 and are along with total NO_y measurements ongoing, PAN measurements were made between March 1997 and April 1998. Measurements of particulate nitrate and HNO_3 were performed during four seasonal field campaigns between July 1997 and April 1998. Because the measurement station and instrumental details have already been described elsewhere (Baltensperger et al., 1997; Weingartner et al., 1999; Zellweger et al., 1999, 2000), only a brief summary of experimental aspects is presented here.

2.1. Measurement site and inlet system

The high alpine research station Jungfraujoch (46°33′ N, 7°59′ E, 3580 m asl) is located on the main crest of the Bernese Alps, Switzerland (e.g. Baltensperger et al., 1997).

ACPD
2, 2259–2296, 2002

Two inlet systems, both located on top of the Sphinx building, were used for the measurements of NO, NO_2, NO_y, HNO_3, particulate nitrate and PAN. HNO_3, particulate nitrate and the aerosol surface area were measured using the GAW aerosol inlet (Weingartner et al., 1999). In addition to the original inlet system, a polyethylene tube of 3 m length (i.d. 4 mm) was used inside the stainless steel tube. The inlet heating (20°C) resulted in low relative humidity (<10%). The sample flow rate was 4 l min^{-1}. NO, NO_2, NO_y, PAN and CO and O_3 were measured using the NABEL stainless steel inlet with an inside diameter (i.d.) of 8 cm and a total length of 3.1 m. The air flow rate was 50 m^3 h^{-1}, and a heating system provided a constant gas temperature of 12°C. NO_x, NO_y and PAN instruments were connected directly to the inlet with PTFE tubing.

2.2. Instrumentation

NO, NO_x and NO_y were measured with a commercially available instrument ($CraNO_x$, Ecophysics) using two chemiluminescence detectors (CLD 770 AL pptv) with temperature-controlled reaction chambers. NO_x was measured as NO after photolytic conversion (PLC 760). NO_y species were converted on a heated gold catalyst (300° C) with 2% CO (99.997%, Messer-Griesheim GmbH) as a reducing agent (Bollinger et al., 1983; Fahey et al., 1985, 1986). A full description of the instrumentation including interferences, conversion efficiencies, statistics and sensitivities can be found in Zellweger et al. (2000). An automatic calibration of the instrument was performed every 23 h. The chemiluminescence detectors were calibrated with NO standard gas (5 ± 0.1 ppmv, diluted with zero air to 30 ppbv) and zero air (dew point −20° C), and the conversion efficiencies of both converters were measured for NO_2 by gas phase titration of NO with ozone. If the conversion efficiency dropped below 95% (∼ every 3 months), the Au catalyst was cleaned with ethanol, acetone and ultrapure water. The conversion efficiencies of the PLC ranged from 45 to 82%. The NO, NO_2 and NO_y impurity of the zero air was checked daily. The NO standard mixture (NO 99.8% in N_2 99.999%, Messer-Griesheim GmbH) was traced back to the National Institute of Standards and Technology (NIST) Reference Material. The instrumental detection limit for NO, NO_2

ACPD
2, 2259–2296, 2002

and NO_y was 50 pptv for 2 min and 20 pptv for 30 min average values, respectively. Overall uncertainties in the measurements were estimated to be ±5% for NO, ±10% for NO_2 and ±9% for NO_y at ambient levels of 500 pptv (1σ). They include the precision of the CLDs, the NO standard uncertainty, the conversion efficiencies of the PLC (after linear detrending) and the Au catalyst, and artifact uncertainties of the zero air check. Our NO_x and NO_y measurements were compared at the JFJ during spring 1998 with measurements of the School of Environmental Sciences, University of East Anglia (UEA), Norwich (UK), to assess the overall measurement uncertainty. The inlet of the UEA custom-built system consisted of a 1/4 inch PFA tube of 0.2 m length. Further details of the UEA instrument are given in Bauguitte (1998). Agreement of both systems was within 10% (Carpenter et al., 2000), with slightly lower values for our system. For the inter-comparison period between 24 March and 5 April 1998, the following linear relationship for a concentration range of 0 to 2 ppbv was found between the two instruments:

EMPA NO_y (pptv) = 0.94 * UEA NO_y (pptv) + 22.9 pptv (r^2 = 0.89).

Slightly lower values in the EMPA system might be attributed to potential losses of HNO_3 in the inlet system. Therefore, the overall uncertainty of NO_y measurements including inlet losses is estimated to be +9/ – 15%.

PAN was measured with a commercially available gas chromatograph (GC) and a calibration unit (Meteorologie Consult GmbH) coupled to an electron capture detection unit (ECD). The instrument and the calibration procedure is described in Zellweger et al. (2000). The detection limit was 50 pptv, and the overall measurement uncertainty was estimated to be ±3% (1σ).

HNO_3 and particulate nitrate measurements were carried out with the wet effluent diffusion denuder/aerosol collector (WEDD/AC) technique described by Blatter et al. (1994) and Simon and Dasgupta (1995). The detection limit was 10 pptv for HNO_3 and particulate nitrate (10 min sampling time). Details of the instrument are described in Zellweger et al. (1999, 2000).

Both CO and O_3 were continuously monitored with commercially available instru-

ments by the NABEL network (APMA-360, Horiba, for CO; Thermo Environmental Instruments, Model 49C, for O_3). The detection limit was 30 ppbv for CO and 0.5 ppbv for O_3 (30 min average). More detailed information including measurement uncertainties and the calibration procedure can be found in Zellweger et al. (2000).

The aerosol active surface area concentration was measured using an epiphaniometer (Gäggeler et al., 1989). This instrument detects the active surface area concentration, which represents the total particle surface area accessible to a diffusing molecule (Baltensperger et al., 2001). The data is corrected for the decline of the actinium source ($T_{1/2}$ = 21.7 years) and was inverted using the algorithm presented in Rogak et al. (1991). The raw data (units: counts per second, cps) were converted into an active surface area concentration ($\mu m^2\,cm^{-3}$) using the algorithm described in (Baltensperger et al., 2001). The relative statistical error of the epiphaniometer signal was found to be 7% for median winter concentrations and negligible for summer concentrations.

2.3. Definition of meteorological filters

Meteorological processes were recognized as playing an important role in the understanding of measurements obtained at elevated continental sites. Therefore, care was taken to identify and separate periods with a potential perturbation due to local or regional pollution sources. The data was divided into two periods, "undisturbed" and "disturbed" free tropospheric (FT) conditions. The term "disturbed FT" is used to account for the various processes involved during dilution of PBL air with FT air during upward transport. For instance, the contribution of PBL to undisturbed FT air masses was estimated at 14–20% during convection events. This corresponds to a dilution factor of ~5 to 7 of PBL air by FT air masses (Zellweger et al., 2000). In this work, disturbed FT conditions are defined as FT air masses that have been mixed with PBL air masses due to any of the following meteorological conditions: (1) föhn (or chinook) events, (2) synoptical lifting (e.g. frontal systems), and (3) thermally induced vertical transport. These three conditions may significantly influence concentrations of gaseous and aerosol parameters and are crucial for the interpretation of time series

obtained at Alpine stations. Data were categorized in the priority (1)>(2)>(3) in order to optimize discrimination, and criteria are further described below.

1. Föhn events were excluded from the FT data using a procedure described by Forrer et al. (2000). In addition to the work of Forrer et al. (2000), north (NF) and south föhn (SF) events were distinguished. The following criteria were used to detect föhn events, in which all criteria had to be fulfilled:
   - The absolute north-south pressure difference over the Alps using data from the Stabio (Southern Switzerland) and Schaffhausen (Northern Switzerland) meteorological stations was >2.1 hPa /100 km according to Hoinka (1980).
   - The relative humidity on the lee side of the Alps using data from Altdorf for south-föhn and Locarno-Monti for north-föhn events was <50%, and accompanied by precipitation at the other station.
   - The local wind speed at the JFJ was >10 m s^{-1}. These criteria were verified by comparison with weather charts, the Swiss Meteorological Institute (SMI) bulletin and 3-D back-trajectories.
2. Synoptical lifting (SYN) (e.g. frontal systems) was excluded from the undisturbed FT data by running 3-D back-trajectories calculated by the TRAJEK DWD-model (Fay et al., 1995) using the wind fields of the Swiss Model (SM). The SM is a hydrostatic numerical weather prediction model with a grid size of ~14 km, which is operationally used at the SMI. The arrival location of the calculated trajectories was the JFJ, and the altitude was set to 700 hPa in the model. The trajectories were then analyzed with respect to their minimum height (corresponding to maximum pressure) 24 h previous to their arrival time. If the trajectory height dropped below the 850 hPa level for at least four hours, the data were excluded from the undisturbed FT data set. These criteria were verified by comparison with data from the Alpine Weather Statistics (AWS) scheme (Schüepp, 1979; Wanner et al., 1998; Forrer et al., 2000).

3. Periods where thermally induced vertical transport (THER) occurred were excluded from undisturbed FT data using the following procedure:

   – Periods with diurnal peak concentrations between 15 February and 15 October were excluded from FT conditions by comparing the mean concentrations of NO_y for the diurnal periods between 03:00 to 09:00 CET on two consecutive days with the period from 15:00 to 21:00 CET between the morning periods. If NO_y was ≥50% higher during the afternoon period, only the data from 03:00 to 09:00 CET was considered to represent undisturbed FT conditions. If no NO_y data was available, the aerosol surface area concentration was used because of its similar diurnal behavior during thermally induced vertical transport at the JFJ (Zellweger et al., 2000). If both NO_y and aerosol surface area concentration data were missing, the specific humidity (q) was used. For q, the criterion for thermally induced vertical transport was a ≥25% higher concentration during the afternoon in comparison to the morning periods (same time intervals as above).

   – Convective days (anticyclonic or indifferent conditions) from March to September with low wind speed at the 500 hPa level were excluded entirely from the FT data. Such periods were shown to be influenced by convective boundary layer (CBL) air masses throughout the whole day (Zellweger et al., 2000).

A map showing the location of the Jungfraujoch and the other stations used for the evaluation of the above described meteorological filters is presented in Fig. 1. The seasons in this work are defined as spring (March to May, summer (June to August), autumn (September to November), and winter (December to February). The winter half year is defined as from September to February.

3. Results and discussion

3.1. Seasonal variation and meteorological transport processes

An overview of monthly median and mean NO_y, NO_x, PAN mixing ratios and the NO_x/NO_y ratio for the period April 1997 to March 1999 is given in Fig. 2 for the entire data set. Generally higher NO_y concentrations were observed at the JFJ during spring and summer, due to enhanced vertical transport processes during these seasons, and in the case of PAN higher production rates within the CBL. The monthly mean values of NO, NO_x and NO_y were often found to be a factor of two or more higher than the corresponding median values due to the occurrence of relatively short episodes with high concentrations. This can be attributed to periods with transport of polluted air masses from source regions to the JFJ caused by various meteorological processes (Zellweger et al., 2000).

Ground-based measurements of NO_y at remote sites are relatively sparse in number, and only few data are available. The NO_y concentrations measured at the JFJ are generally higher compared to those at other remote sites. Fischer et al. (1998) reported NO_y measurements at the Izaña Observatory on Tenerife Island. During the Oxidizing Capacity of the Tropospheric Atmosphere (OCTA) campaign, nighttime mean NO_y concentrations of 370 to 420 pptv were reported. This is slightly below the NO_y level of mean 653 pptv that is observed during summer for undisturbed FT conditions at the JFJ. The lowest values that have been measured at Izaña are as low as 120 pptv, which is comparable to the lowest values observed at the JFJ during undisturbed FT conditions. At Izaña thermally induced vertical transport was also recognized as playing an important role in the upward transport of polluted air masses. However, the difference between the "polluted" daytime conditions of Izaña with a reported mean NO_y of 520 to 1300 pptv is often less pronounced compared to the JFJ (mean summer NO_y of 899 pptv during polluted conditions). The period when high daytime NO_y of 1300 pptv was reported at Izaña was associated with air parcels of continental origin. NO_y mixing ratios at this or a higher level are also often observed at the JFJ, indicating

ACPD
2, 2259–2296, 2002

anthropogenic influences.

Another important contribution to NO_y measurements was made by Munger et al. (1996) for the remote site Schefferville in Canada (elevation 500 m) where summertime NO_y averaged 308 pptv. This appears to be representative of background NO_y levels in the boundary layer far from emission sources, and is comparable to undisturbed FT conditions at the JFJ.

Recent work by Thornberry et al. (2001) reported NO_y measurements and speciation made during the PROPHET summer intensive at a rural site along the boundary of Cheboygan and Emmet Counties, USA (45°30′ N, 84°42′ W, elevation 238 m). Air mass origin over the PROPHET site oscillated between relatively clean regions in the north and regions of greater anthropogenic emissions to the south, and higher mixing ratios of NO_y species were generally associated with southerly transport. NO_y averaged 2.9 ppbv during southerly flow, and 0.9 ppbv during "clean" northerly flow respectively. However, the variability of the NO_y mixing ratios was high for both flow regimes. Periods with average NO_y well below 500 pptv were also observed at the PROPHET site, which is comparable to other remote sites and the undisturbed FT at the JFJ. Furthermore, a typical diurnal pattern with nighttime maximum was also observed at the PROPHET site, which was explained by vertical mixing of pollutants from the nocturnal boundary layer into the overlying residual layer after sunrise. In the following, the influence of different meteorological situations on the JFJ data set is investigated. Figure 3 shows the frequencies of the meteorological situations described in Sect. 2.3 for the winter (September to February) and summer (March to August) half-year of the period from April 1997 to March 1999. As expected, thermally induced vertical transport occurs predominately during spring and summer, whereas frontal systems and föhn events occur all year round.

Table 1 gives an overview of seasonal median and mean NO_x, NO_y, PAN, HNO_3, particulate nitrate, CO, O_3 and the aerosol surface area concentration measured at the JFJ for the period from April 1997 to March 1999. Table 1 includes the whole data set based on hourly values, as well as for undisturbed FT conditions, and disturbed FT

conditions. It can be seen from Table 1 that the NO_y mixing ratio is comparable during the spring and summer months (median NO_y 766 pptv and 702 pptv, all data) and during the autumn and winter months (median NO_y 495 pptv and 411 pptv, all data). This is also the case for the NO_x and PAN mixing ratios, while the aerosol surface area concentration, particulate nitrate and nitric acid showed maximum concentrations during the summer months. The effect of data filtering for NO_x, NO_y, PAN and the aerosol surface area concentration is illustrated in Figs. 4a and b, where monthly median mixing ratios are shown for the filtered data set as well as for föhn events, synoptical lifting and thermally induced vertical transport. It can be seen that the meteorological processes described in Sect. 2.3 caused an increase of the mixing ratios as well as of the variability for NO_x, NO_y and PAN. The effect was most pronounced for NO_x as a primary pollutant with a strong vertical concentration gradient. Different behavior was observed for the aerosol surface area concentration, where higher values were observed only for thermally induced vertical transport. The lower values for the aerosol surface area concentration during föhn events and synoptical lifting can be explained by precipitation scavenging during these transport events. This mechanism is the major sink for particulate matter as well as for the highly water soluble nitric acid. Thus, the summer maximum of aerosol parameters, particulate nitrate and HNO_3 can be explained by episodes with thermally induced vertical transport processes, when wet deposition is of minor importance.

Frequency distributions of NO_x, NO_y, the NO_x/NO_y ratio, PAN, the aerosol surface area concentration, and CO are shown in Figs. 5a and b. For each species, undisturbed FT conditions, north and south föhn events, synoptical lifting and thermally induced vertical transport data are shown separately. The plots in Figs. 5a and b are based on hourly mean values, and for each species the data was divided into 50 bins.

It can be seen from Figs. 5a and b that the mixing ratios of NO_x, NO_y, CO, PAN and the NO_x/NO_y ratio were elevated during south föhn events, in conjunction with low aerosol concentrations. Similar increases of the CO and NO_x mixing ratios at the JFJ during south föhn episodes were also observed by Forrer et al. (1999) for the period

between April 1996 and November 1997. During the observation period between April 1997 and March 1999, 4.1% of the data fulfilled the criteria for south föhn. Although these events are less frequent than thermally induced vertical transport or synoptical lifting, they may significantly add to the upward transport of gaseous species over the Alpine region. Forrer et al. (1999) showed by trajectory analysis that air masses reaching the JFJ during south föhn episodes from the south and southeast seem to be frequently below the 900 hPa level and are therefore likely to be influenced by sources from this region. The influence of source regions during south föhn events can also be seen from the present data set, where a median NO_x mixing ratio of 0.5 ppbv was observed during south föhn events, with 11% of the data being above 2.5 ppbv. This is significantly higher compared to undisturbed FT values with a median NO_x mixing ratio of 0.11 ppbv. The NO_x/NO_y ratio was also significantly higher during south föhn events compared to the undisturbed FT. In contrast, only a very low aerosol surface area concentration was observed, which can be explained by wet deposition.

Similar behavior was observed for north föhn events, which occurred with a frequency of ~5% between April 1997 and March 1999. Figures 5a and b show that the NO_x/NO_y ratio was comparable to south föhn events, in conjunction with low aerosol surface area concentrations. However, the mixing ratios of gaseous species (NO_x, PAN, total NO_y) were lower compared to south föhn events. Explanations for this may be the different pollution levels north (Swiss plateau) and south (Po basin) of the Alps as well as the orographic situation of the Alps.

Synoptical lifting (e.g. frontal systems) is another important transport process for NO_y species, which may be enhanced by Alpine orography. It can be seen from Figs. 5a and b that air rich in NO_x, NO_y, PAN and CO was transported to the JFJ during synoptical lifting. The frequency distributions of these compounds during synoptical lifting are comparable to north föhn events. In contrast to föhn events, the aerosol surface area concentration increased slightly. This may be explained by better vertical mixing and less precipitation during synoptical lifting.

Thermally induced vertical transport also leads to increased NO_y and aerosol surface

ACPD
2, 2259–2296, 2002

area concentrations (see Figs. 5a and b). Thermally induced vertical transport has been recognized as an important mechanism of upward transport to the JFJ for aerosol particles (Baltensperger et al., 1997; Lugauer et al., 1998, 2000; Nyeki et al., 1998, 2000), as well as for gaseous species (Zellweger et al., 2000).

The identification of thermally induced vertical transport was based on the diurnal variation of NO_y, the aerosol surface area concentration, and the specific humidity (see Sect. 2.3). This is in contrast to earlier studies (Lugauer et al., 1998, 2000) where thermally induced transport was determined according to the Alpine Weather Statistics (AWS) scheme (Schüepp, 1979; Wanner et al., 1998). Convective AWS days during spring and summer usually exhibit a pronounced diurnal cycle with afternoon peak concentrations for both aerosol and some gaseous parameters. However, a strong diurnal variation was also observed on several non-convective days according to the AWS classification (e.g. 31 March 1998, AWS Advective type). This might be due to the fact that the AWS classification covers the whole Alpine region and does not account for local wind systems. Figure 6 illustrates diurnal variations of the median NO_y, O_3, and aerosol surface area concentration over the four seasons at the JFJ for days with thermally induced vertical transport and for the undisturbed FT. The aerosol surface area concentration and NO_y showed a distinct diurnal cycle with afternoon maximum concentrations at ~18:00 CET during days with thermally induced vertical transport. A detailed overview of diurnal cycles is given in Lugauer et al. (1998) and Nyeki et al. (1998) for aerosol parameters. The diurnal cycle of radon daughters was described recently (Lugauer et al., 2000). Ozone showed only a very weak diurnal variation for days with thermally induced vertical transport during spring, and no diurnal variation was observed for the rest of the year. This can be explained by small vertical concentration gradients in combination with dilution by FT air during convective transport. Figure 5a shows that the lowest NO_x/NO_y ratios of 0.22 on average were observed during thermally induced upward transport at the JFJ. This supports the conclusion that photochemically well-processed air masses reach the JFJ during spring and summer afternoons. Thus, the NO_x mixing ratios during these periods were comparable to

values of the undisturbed FT, whereas a significant increase of the NO_y mixing ratios was observed.

3.2. Air mass aging

The fact that lower NO_x/NO_y ratios were observed during thermally induced upward transport compared to undisturbed FT conditions at the JFJ suggests that the NO_x/NO_y ratio is not always a suitable parameter to estimate the processing that has occurred in an air parcel. This is especially the case for remote locations, where deposition (e.g. wet and dry deposition of HNO_3) and decomposition processes (e.g. thermal decay of PAN) can make the ratio difficult to interpret. The NO_x/NO_y ratio accounts for the photochemical processing that has occurred in an air parcel. The photochemical aging of an air parcel may be fast, with NO_x/NO_y ratios <0.4 within a few hours (Thornberry et al., 2001). Thus, this ratio may be used to assess the photochemical processing close to sources and on a time scale of less than one day. An alternative parameter to assess the aging process that has occurred in an air parcel is the NO_y/CO ratio, which accounts for both deposition and dilution effects. Close to anthropogenic sources, the NO_x/CO ratio averages ~0.1, whereas values of ~0.005 are observed in the upper troposphere (Jaeglé et al., 1998). However, it should be noted that the NO_y/CO ratio also shows a seasonal variation, with lower values during the winter months due to a longer lifetime of CO. Figure 7 shows seasonal plots of the NO_x/NO_y versus NO_y/CO ratios for different meteorological situations described in Sect. 2.3 and the undisturbed FT. It can be seen that undisturbed FT conditions are always accompanied by the lowest NO_y/CO ratios, indicating advanced aging of these air masses. This ratio may therefore be an alternative method to distinguish between disturbed and undisturbed FT conditions at the JFJ.

A further illustration of the effect of different meteorological situations on the NO_x/NO_y and NO_y/CO ratios is shown in Figs. 8 and 9, where mixing ratios of individually measured NO_y species as well as total NO_y, the NO_x/NO_y and the NO_y/CO ratios and the aerosol surface area concentration are presented for two selected peri-

ods in winter and spring 1998. The periods experiencing south föhn, synoptical lifting and thermally induced vertical transport are also shown in Figs. 8 and 9 (no situation with north föhn occurred during these periods). Again the NO_y/CO ratio increased on average during the above meteorological events. A period of particular interest is during thermally induced vertical transport on 30 March to 1 April (see red highlighted area in Fig. 9). On these days NO_y/CO ratios exceeded 0.01 during the peak in afternoon concentrations, indicating a "pollution" event. In contrast, NO_x/NO_y ratios were very low (below 0.2), which indicates photo-chemically well-processed air masses. The peaks can also be observed in the aerosol surface area concentration, which typically occurs during thermally induced transport processes.

A second interesting period occurred between 3 April and 16 April when several south föhn events were experienced (see yellow highlighted area in Fig. 9). Again, all these events were accompanied by NO_y/CO ratios exceeding 0.01. In contrast to thermally induced transport, NO_x/NO_y ratios also reached high values (approx. 0.7–0.9) during the föhn events. This can be attributed to the high NO_x concentrations observed during these periods. Particle concentrations were relatively low during these föhn events, indicating wet deposition.

3.3. NO_y partitioning – case studies

Summertime NO_y speciation at the JFJ has already been discussed by Zellweger et al. (2000). The most abundant NO_y species was PAN with an average contribution of 36%, followed by NO_x with 22%, particulate nitrate with 17% and HNO_3 with 7%. The sum of NO_x, HNO_3, particulate nitrate and PAN contributed on average 82% to the total NO_y mixing ratio. However, it should be emphasized that an accurate determination of total NO_y with individually measured species is difficult due to measurement uncertainties. Furthermore, the presence of reactive nitrogen compounds which are present in significant quantities but which are not measured in a given data set may also lead to an underestimation of total NO_y.

The NO_y partitioning for selected periods is shown in Figs. 10a–c. During the undis-

turbed FT period from 12–13 February 1998 (Fig. 10a), the NO_x fraction was, at 46%, the most abundant NO_y species, followed by PAN (20%), HNO_3 (9%) and particulate nitrate (3%). An average fraction of 22% could not be identified, and total NO_y averaged 209 pptv. This period can be considered as representative of clean conditions during the autumn and winter months, since total NO_y remained almost constant throughout February 1998 with the exception of the periods when synoptical lifting and thermally induced vertical transport was observed. During periods influenced by synoptical lifting (22–23 February 1998, 07:00–19:00, Fig. 10b), PAN was the most abundant NO_y species (38%), followed by NO_x (26%), HNO_3 (1%) and particulate nitrate (1%). The peak concentration of NO_y was more than 10 times higher during this period compared to the "clean" period, and mainly PAN together with an unidentified fraction was transported to the JFJ. The very low contribution of inorganic nitrate to total NO_y during synoptical lifting can be explained by wet deposition. The period between 27 March and 2 April 1998 (Fig. 10c) was characterized by clean conditions until the morning of 30 March. During this period, an average NO_y mixing ratio of 350 pptv was observed with PAN (39%) as the most abundant NO_y species, followed by NO_x (24%) and inorganic nitrate (4%). Thermally induced vertical transport occurred on the three following days, where very high NO_y mixing ratios were found. On the first day, a maximum NO_y concentration of 3.3 ppbv was observed. During this peak event, NO_y consisted mainly of PAN (42%), followed by particulate nitrate (13%), NO_x (9%) and HNO_3 (3%). In the following night, the air was replaced by undisturbed FT-influenced air, and low concentrations were observed. A very high injection of NO_y was then observed on 31 March with a maximum concentration of 6.9 ppbv, which consisted mainly of particulate nitrate (52%), PAN (30%) and NO_x (5%). HNO_3 was below the detection limit during this episode, indicating that the formation of particulate nitrate was favored due to neutralization of HNO_3. The NO_y rich air was again replaced through horizontal advection during the following night. On 1 April, another thermally induced injection was observed. The NO_y mixing ratio reached 4.7 ppbv, and consisted mainly of PAN (34%), followed by particulate nitrate (20%), NO_x (10%) and HNO_3 (1%). However,

ACPD
2, 2259–2296, 2002

the following advection of clean air was not effective enough to replace the injected air mass completely by FT air, leading to elevated NO_y mixing ratios during the night of 2 April. This phenomenon was already observed during summer 1997 for convective days with low wind speed at the 500 hPa level (Zellweger et al., 2000). Figure 11 summarizes levels and speciation of NO_y during selected periods. The NO_y mixing ratio remained relatively constant during undisturbed FT periods. Highest NO_y mixing ratios were observed during spring, but the seasonal difference between summer and winter was small. However, differences can be seen in the NO_y speciation. The NO_x/NO_y ratio was highest during winter (0.46) and lowest during spring (0.21). This reflects the lower photochemical activity during the winter months. By similar reasons, PAN/NO_y was highest during spring (0.39) and lowest during winter (0.20). Meteorological processes also have a strong influence on the level and speciation of NO_y. The NO_y speciation for selected periods (thermally induced vertical transport, föhn, frontal systems) is also shown in Fig. 11. The NO_y mixing ratio reached an average level of 1 to 4 ppbv, a factor 4 to 10 higher compared to undisturbed FT conditions. The NO_x/NO_y ratio was lowest during episodes with thermally induced vertical transport, accompanied by high NO_3^-/NO_y and PAN/NO_y ratios. This again reflects the photochemical transformation of NO_x during thermally induced upward transport, yielding a photochemically aged air upon arrival at the Jungfraujoch. The low NO_x/NO_y and the high PAN/NO_y ratios also suggest that PAN degradation is not a major source of NO_x at the JFJ. Rather, the Alpine region appears to be a passive transport pathway of PAN (and other NO_y compounds), which is in line with recent results from FREETEX'98 (Carpenter et al., 2000).

4. Conclusions

Speciated and total NO_y were measured at the high-alpine site Jungfraujoch (JFJ) over a two-year period. The NO_y mixing ratios and partitioning strongly depended on meteorological conditions. As a consequence, filters must be used at Alpine (and

presumably other continental) sites to distinguish between undisturbed and disturbed FT conditions. Attempts to develop a filter procedure for the combined European GAW virtual baseline station, comprising the Jungfraujoch (Switzerland), the Sonnblick (Austria) and the Zugspitze (Germany) high-alpine stations, have not been successful so far (Fricke et al., 2000).

This study presents filters based mainly on meteorological parameters for the Jungfraujoch station. The meteorological processes that were identified to influence NO_y mixing ratios and composition include föhn (both from north and south), synoptical lifting (e.g. fronts) and thermally induced vertical transport. Highest NO_y mixing ratios were observed during south föhn events. This is in contrast to aerosol parameters, for which thermally induced vertical transport is the major process for upward transport. Seasonal variation in the composition of NO_y was found, with PAN being dominant during spring and summer, and NO_x during autumn and winter. The NO_x/NO_y ratio reached the lowest values during thermally induced upward transport. As a consequence, the NO_x/NO_y ratio is not a suitable parameter to estimate the air mass aging at remote sites. Alternatively, the NO_y/CO ratio proved to be an interesting new approach in assessing the age of an air mass.

Acknowledgement. The support of the international foundation for high-alpine research stations Jungfraujoch and Gornergrat (HFSJG) is highly appreciated. This work was supported by the Swiss Meteorological Institute (MeteoSwiss) and the Global Atmosphere Watch (GAW) program, as well as the Swiss Agency for Environment, Forests and Landscape (BUWAL) which provided the NABEL data.

References

Baltensperger, U., Gäggeler, H. W., Jost, D. T., Lugauer, M., Schwikowski, M., Seibert, P., and Weingartner, E.: Aerosol climatology at the high-alpine site Jungfraujoch, Switzerland, J. Geophys. Res., 102, 19 707–19 715, 1997.

Baltensperger, U., Weingartner, E., Burtscher, H., and Keskinen, J.: Dynamic Mass and Surface Area Measurements, in: Measurement Technology, (Eds) Baron, P. A. and Willeke, K., John Wiley and Sons, New York, 2nd ed., 387–418, 2001.

Bauguitte, S.: in TACIA Final Report, EC R & D Programme Environment and Climate, 21–26, 1998.

Berkowitz, C. M., Fast, J. D., Springston, S. R., Larsen, R. J., Spicer, C. W., Doskey, P. V., Hubbe, J. M., and Plastridge, R.: Formation mechanisms and chemical characteristics of elevated photochemical layers over the northeast United States, J. Geophys. Res., 103, 10 631–10 647, 1998.

Blatter, A., Neftel, A., Dasgupta, P. K., and Simon, P. K.: A combined wet effluent denuder and mist chamber system for deposition measurements of NH_3, NH_4^+, HNO_3 and NO_3^-, in: Physicochemical Behaviour of Atmospheric Pollutants, (Eds) Angeletti, G. and Restelli G., European Commission, Brussels, 767–772, 1994.

Bollinger, M. J., Sievers, R. E., Fahey, O. W., and Fehsenfeld, F. C.: Conversion of nitrogen dioxide, nitric acid, and n-propyl nitrate to nitric oxide by gold-catalyzed reduction with carbon monoxide, Anal. Chem., 55, 1980–1986, 1983.

Carpenter, L. J., Green, T., Mills, G., Penkett, S. A., Zanis, P., Schuepbach, E., Monks, P. S., and Zellweger, C.: Oxidised nitrogen and ozone production efficiencies in the springtime free troposphere of the Alps, J. Geophys. Res., 105, 14 547–14 559, 2000.

Carroll, M. A. and Thompson, A. M.: NO_x in the non-urban troposphere, in: Progress and Problems in Atmospheric Chemistry, (Ed) Barker, J. R., World Sci., vol. 3, Singapore, 1995.

Crutzen, P. J.: The role of NO and NO_2 in the chemistry of the troposphere and stratosphere, Ann. Rev. Earth Planet Sci., 7, 443–472, 1979.

Fahey, D. W., Eubank, C. S., Hübler, G., and Fehsenfeld, F. C.: Evaluation of a catalytic reduction technique for the measurement of total reactive odd-nitrogen NO_y in the atmosphere, J. Atmos. Chem., 3, 435–468, 1985.

Fahey, D. W., Hübler, G., Parrish, D. D., Williams, E. J., Norton, R. B., Ridley, B. A., Singh, H. B., Liu, S. C., and Fehsenfeld, F. C.: Reactive nitrogen species in the troposphere: Measurements of NO, NO_2, HNO_3, particulate nitrate, PAN, O_3 and total reactive odd nitrogen (NO_y) at Niwot Ridge, Colorado, J. Geophys. Res., 92, 14 710–14 722, 1986.

Fay, B., Glaab, H., Jacobsen, I., and Schrodin, R.: Evaluation of eulerian and lagrangian atmosphere transport models at the Deutscher Wetterdienst using ANATEX surface tracer data, Atmos. Environ., 29, 2485–2497, 1995.

Fischer, H., Nikitas, C., Parchatka, U., Zenker, T., Harris, G. W., Matuska, P., Schmitt, R., Mihelcic, O., Muesgen, P., Paetz, H.-W., Schulz, M., and Volz-Thomas, A.: Trace gas measurements during the oxidizing capacity of the tropospheric atmosphere campaign 1993 at Izaña, J. Geophys. Res., 103, 13 505–13 518, 1998.

Forrer, J., Rüttimann, R., Schneiter, D., Fischer, A., Buchmann, B., and Hofer, P.: Variability of trace gases at the high Alpine site Jungfraujoch caused by meteorological transport processes, J. Geophys. Res., 105, 12 241–12 251, 2000.

Fricke, W., Fischer, A., Forrer, J., Gilge, S., Hofer, P., Jeannet, P., Kaiser, A., Klennoff, K., Nemeth, R., Ries, L., and Winkler, P.: Filterung luftchemischer Messreihen im Alpenraum zur Charakterisierung ihrer Representanz, Berichte des Deutschen Wetterdienstes, No. 211, (in German), 2000.

Gäggeler, H. W., Baltensperger, U., Emmenegger, M., Jost, D. T., Schmitt-Ott, A., Haller, P., and Hofmann, M.: The epiphaniometer, a new device for continuous aerosol monitoring, J. Aerosol Sci., 20, 557–564, 1989.

Hoinka, K. P.: Synoptic-scale atmospheric features and föhn, Contr. Atmos. Phys., 53, 485–507, 1980.

Jaeglé, L., Jacob, D. J., Wang, Y., Weinheimer, A. J., Ridley, B. A., Campos, T. L., Sachse, G. W., and Hagen, D. E.: Sources and chemistry of NO_x in the upper troposphere over the United States, Geophys. Res. Lett., 25, 1705–1708, 1998.

Lugauer, M., Baltensperger, U., Furger, M., Gäggeler, H. W., Jost, D. T., Schwikowski, M., and Wanner, H.: Aerosol transport to the high alpine sites Jungfraujoch (3454 m asl) and Colle Gnifetti (4452 m asl), Tellus, 50B, 76–92, 1998.

Lugauer, M., Baltensperger, U., Furger, M., Gäggeler, H. W., Jost, D. T., Nyeki, S., and Schwikowski, M.: Influences of vertical transport and scavenging on aerosol particle surface area and radon decay product concentrations at the Jungfraujoch (3454 m above sea level), J. Geophys. Res., 105, 19 869–19 879, 2000.

Munger, J. W., Wolfsy, S. C., Bakwin, P. S., Fan, S.-M., Goulden, M. L., Daube, B. C., and Goldstein, A. H.: Atmospheric deposition of reactive nitrogen oxides and ozone in a temperate deciduous forest and a subarctic woodland, 1. Measurements and mechanisms, J. Geophys. Res., 101, 12 693–12 657, 1996.

Nyeki, S., Baltensperger, U., Colbeck, I., Jost, D. T., Weingartner, E., and Gäggeler, H. W.: The Jungfraujoch high-alpine research station (3454 m) as a background clean continental site for the measurement of aerosol parameters, J. Geophys. Res., 103, 6097–6107, 1998.

Nyeki, S., Kalberer, M., Colbeck, I., De Wekker, S., Furger, M., Gäggeler, H. W., Kossmann, M., Lugauer, M., Steyn, D., Weingartner, E., Wirth, M., and Baltensperger, U.: Convective boundary layer evolution to 4 km asl over high-alpine terrain: Airborne lidar observations in the Alps, Geophys. Res. Lett., 27, 689–692, 2000.

Roberts, J. M.: Reactive odd-nitrogen (NO_y) in the atmosphere, in: Composition, Chemistry and Climate of the Atmosphere, (Ed) Singh, H. B., Van Nostrand Reinhold, 176–215, 1995.

Rogak, S. N., Baltensperger, U., and Flagan, R. C.: Measurements of mass transfer to agglomerate aerosol, Aerosol Sci. Technol. 14, 447–458, 1991.

Schüepp, M.: Witterungsklimatologie der Schweiz, Band III, Beilage zu den Annalen 1978, (in German), 94 pp, Available from Swiss Meteorological Institute, 8044 Zürich, Switzerland, 1979.

Simon, P. K. and Dasgupta, P. K.: Continuous automated measurement of gaseous nitrous and nitric acids and particulate nitrite and nitrate. Environ. Sci. Technol. 29, 1534–1541, 1995.

Thornberry, T., Carroll, M. A., Keeler, G. J., Sillman, S., Bertman, S. B., Pippin, M. R., Ostling, K., Grossenbacher, J. W., Shepson, P. B., Cooper, O. R., Moody, J. L., and Stockwell, W. R.: Observations of reactive oxidized nitrogen and speciation of NO_y during the PROPHET summer 1998 intensive, J. Geophys. Res., 106, 24 359–24 386, 2001.

Wanner, H., Salvisberg, E., Rickli, R., and Schüepp, M.: 50 years of Alpine Weather Statistics (AWS), Meteorol. Zeitschrift, 7, 99–111, 1998.

Weingartner, E., Nyeki, S., and Baltensperger, U.: Seasonal and diurnal variation of aerosol size distributions ($10 < D < 750$ nm) at a high-alpine site (Jungfraujoch 3580 m asl), J. Geophys. Res., 104, 26 809–26 820, 1999.

Zellweger, C., Ammann, M., Baltensperger, U., and Hofer, P.: NO_y speciation with a combined wet effluent diffusion denuder-aerosol collector coupled to ion chromatography, Atmos. Environ., 33, 1131–1140, 1999.

Zellweger, C., Ammann, M., Buchmann, B., Hofer, P., Lugauer, M., Rüttimann, R., Streit, N., Weingartner, E., and Baltensperger, U.: Summertime NO_y Speciation at the Jungfraujoch, 3580 m asl, Switzerland, J. Geophys. Res., 105, 6655–6667, 2000.

Table 1. Seasonal median and mean values of NO_x, NO_y, PAN, HNO_3, particulate nitrate, CO, O_3, and the aerosol surface area (AS) concentration with standard deviation (s.d.) and number of measurements (*N*) based on hourly values at the JFJ for the period from April 1997 to March 1999, for the whole data set, as well as for undisturbed and disturbed FT conditions. (Spring MAM = March to May, etc.)

	All Data				Undisturbed FT				Disturbed FT			
	Median	Mean	s.d.	N	Median	Mean	s.d.	N	Median	Mean	s.d.	N
Spring MAM												
NO_x [pptv]	152	370	769	3860	98	183	289	1631	204	506	958	2229
NO_y [pptv]	766	1103	1076	3978	581	748	614	1693	981	1365	1255	2285
PAN [pptv]	294	346	245	2828	256	287	212	1192	334	389	258	1636
HNO_3 [ppt]	10	18	19	420	5	17	20	182	14	20	19	238
NO_3^- [pptv]	5	269	754	206	5	24	46	81	5	427	935	125
CO [ppbv]	168	174	35	4378	160	165	28	1875	173	181	38	2503
O_3 [ppbv]	58	58	9	4316	57	57	8	1847	59	59	9	2469
AS [μm^2 cm^{-3}]	8	14	17	3489	8	13	16	1511	8	14	18	1978
Summer JJA												
NO_x [pptv]	161	206	335	3144	133	191	482	1185	177	215	199	1959
NO_y [pptv]	702	806	538	3239	529	653	570	1225	822	899	495	2014
PAN [pptv]	330	355	211	1804	271	286	198	637	369	393	209	1167
HNO_3 [pptv]	19	70	180	817	17	41	96	235	22	82	203	582
NO_3^- [pptv]	122	161	147	812	68	116	121	275	130	173	155	573
CO [ppbv]	126	129	28	4288	122	125	28	1592	128	131	27	2696
O_3 [ppbv]	59	58	9	4261	58	57	10	1587	59	58	8	2674
AS [μm^2 cm^{-3}]	13	19	17	4151	10	16	16	1565	15	21	18	2586
Autumn SON												
NO_x [pptv]	143	276	494	2234	115	205	355	1289	184	373	624	945
NO_y [pptv]	495	738	869	3626	422	553	477	2269	700	1049	1221	1351
PAN [pptv]	118	145	124	1456	102	119	81	983	142	200	171	473
HNO_3 [pptv]	5	17	33	765	5	18	36	628	5	11	15	137
NO_3^- [pptv]	5	12	13	761	5	11	14	624	15	15	9	137
CO [ppbv]	143	149	40	4190	138	146	40	2539	149	154	39	1651
O_3 [ppbv]	49	49	7	4176	49	49	7	2541	50	50	8	1635
AS [μm^2 cm^{-3}]	5	10	13	2258	5	7	7	1342	7	15	17	916
Winter DJF												
NO_x [pptv]	115	320	565	2281	87	203	454	1636	409	617	695	643
NO_y [pptv]	411	673	797	2997	350	501	659	2233	911	1178	939	764
PAN [pptv]	115	154	156	1453	105	132	105	1078	149	219	239	375
HNO_3 [pptv]	11	14	15	762	10	13	14	697	19	26	23	65
NO_3^- [pptv]	11	20	63	763	11	19	64	697	18	31	39	66
CO [ppbv]	171	179	46	3248	164	169	41	2409	191	207	49	839
O_3 [ppbv]	46	46	7	4027	47	47	7	3038	43	42	7	989
AS [μm^2 cm^{-3}]	6	9	13	4267	6	9	13	3157	7	11	14	1110

ACPD
2, 2259–2296, 2002

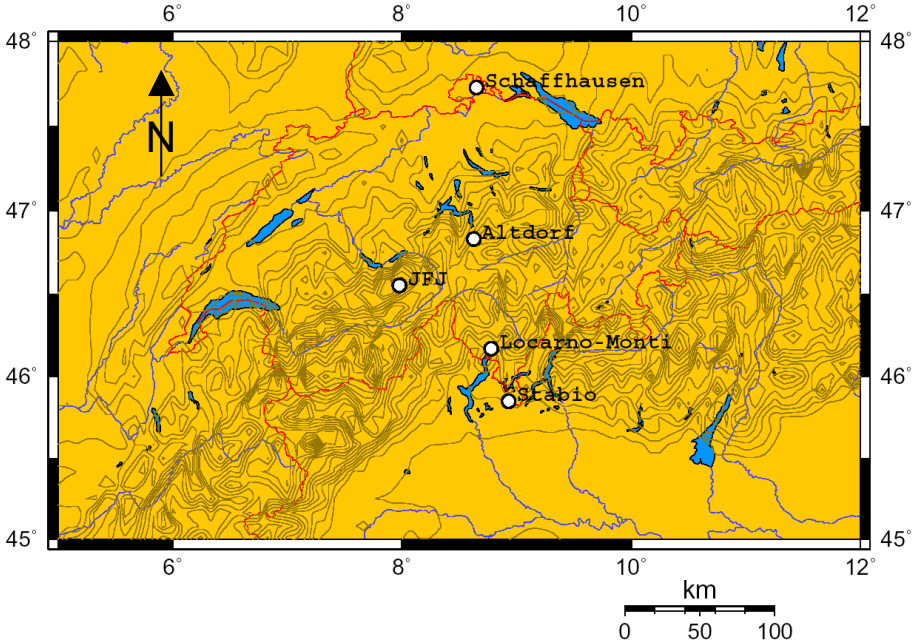

Fig. 1. Map showing the location of the Jungfraujoch and the other stations used for the definitions of the meteorological filters.

ACPD

2, 2259–2296, 2002

Partitioning of NO_y and dependence of meteorological conditions

C. Zellweger et al.

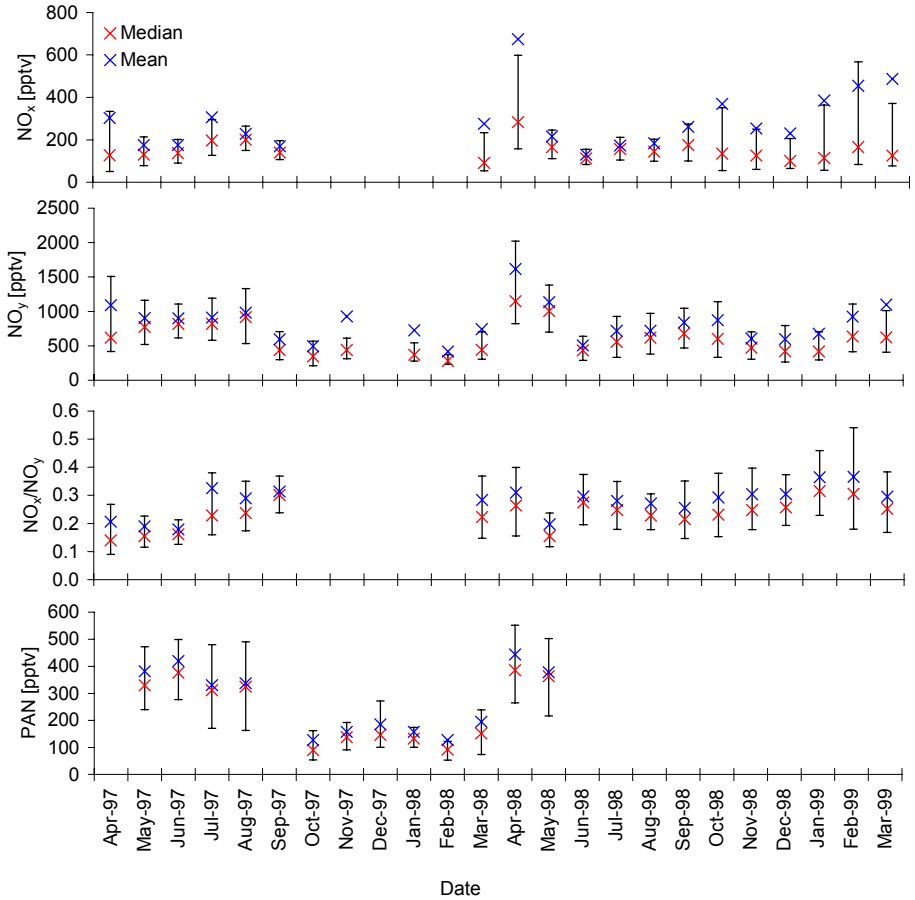

Fig. 2. Monthly mean and median values of NO_y, NO_x, NO, PAN, O_3 and the NO_x/NO_y ratio from April 1997 to March 1999. The first and third quartiles are indicated by bars. Only data where >75% of the hourly values were available are shown.

ACPD
2, 2259–2296, 2002

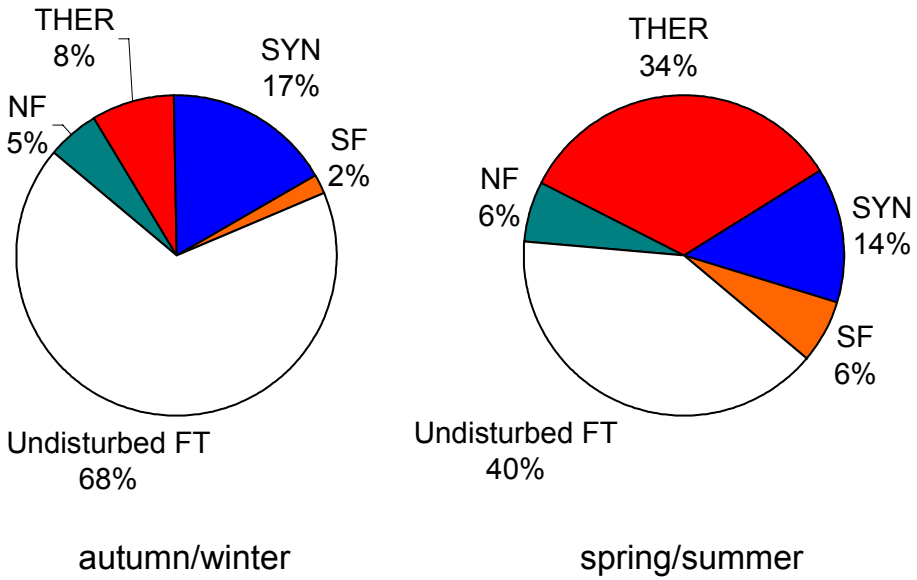

Fig. 3. Frequencies of meteorological situations (NF = north föhn, SF = south föhn, THER = thermally induced vertical transport, SYN = synoptical lifting) for the period between April 1997 and March 1999. Results shown for autumn/winter (September to February) and spring/summer (March to August) half-year periods.

ACPD
2, 2259–2296, 2002

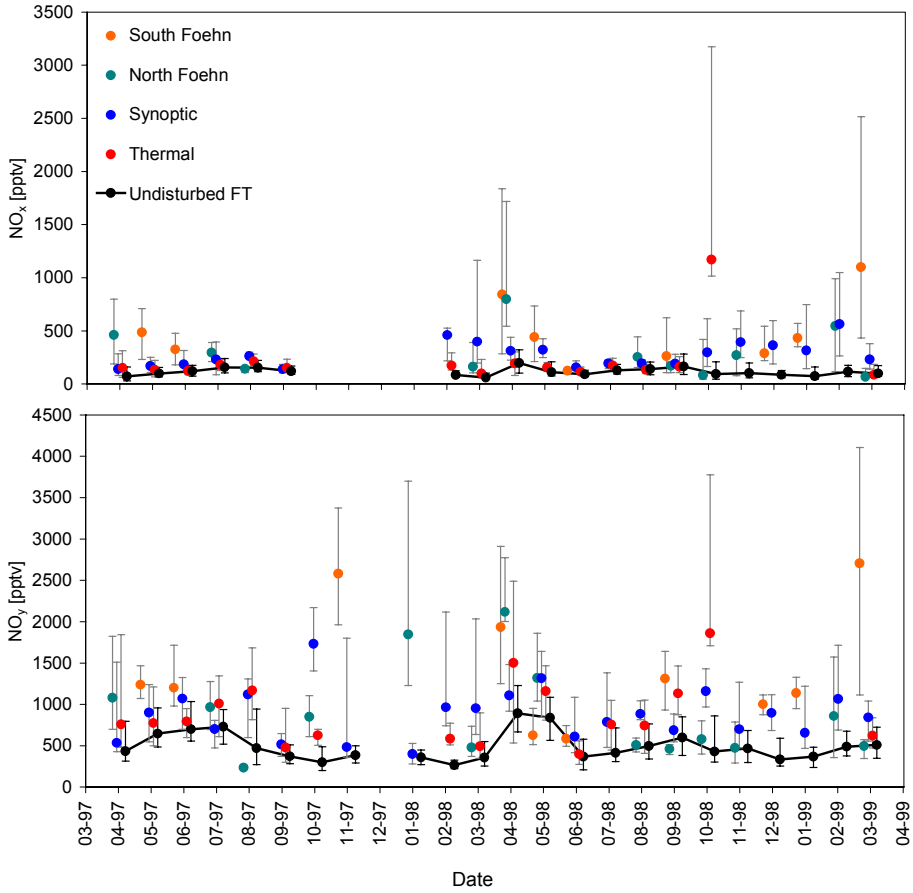

Fig. 4a. Monthly median values of NO_x and NO_y concentration for the filtered data set as well as for different meteorological situations from April 1997 to March 1999. The first and third quartiles are indicated by bars.

ACPD
2, 2259–2296, 2002

Partitioning of NO_y and dependence of meteorological conditions

C. Zellweger et al.

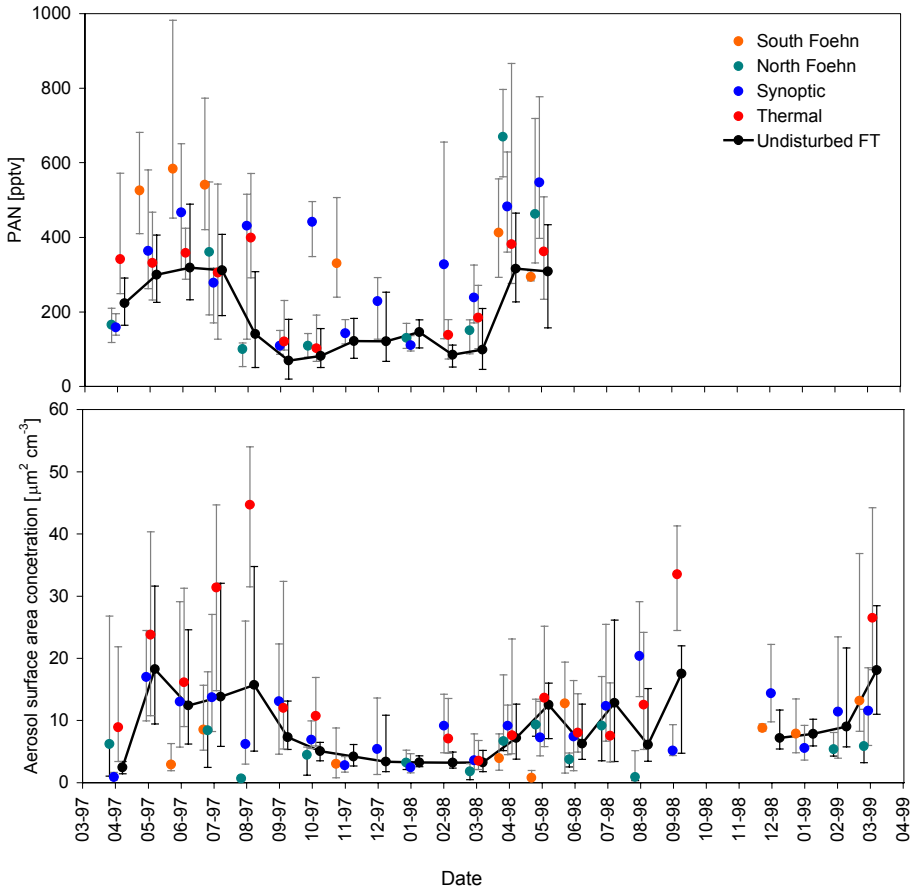

Fig. 4b. Monthly median values of PAN and the aerosol surface area concentration for the filtered data set as well as for different meteorological situations from April 1997 to March 1999. The first and third quartiles are indicated by bars.

ACPD
2, 2259–2296, 2002

Partitioning of NO_y and dependence of meteorological conditions

C. Zellweger et al.

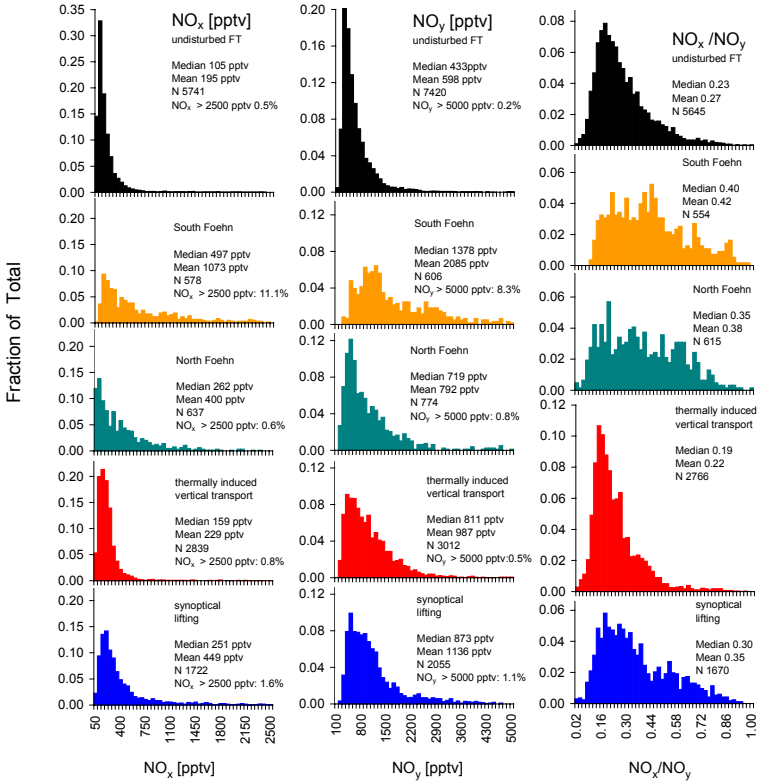

Fig. 5a. Frequency distributions including median, mean and number (N) of values for NO_x, NO_y and the NO_x/NO_y ratio from April 1997 to March 1999 for the whole data set and different meteorological situations. For each species, the data set was based on hourly values and divided into 50 bins.

ACPD
2, 2259–2296, 2002

Partitioning of NO_y and dependence of meteorological conditions

C. Zellweger et al.

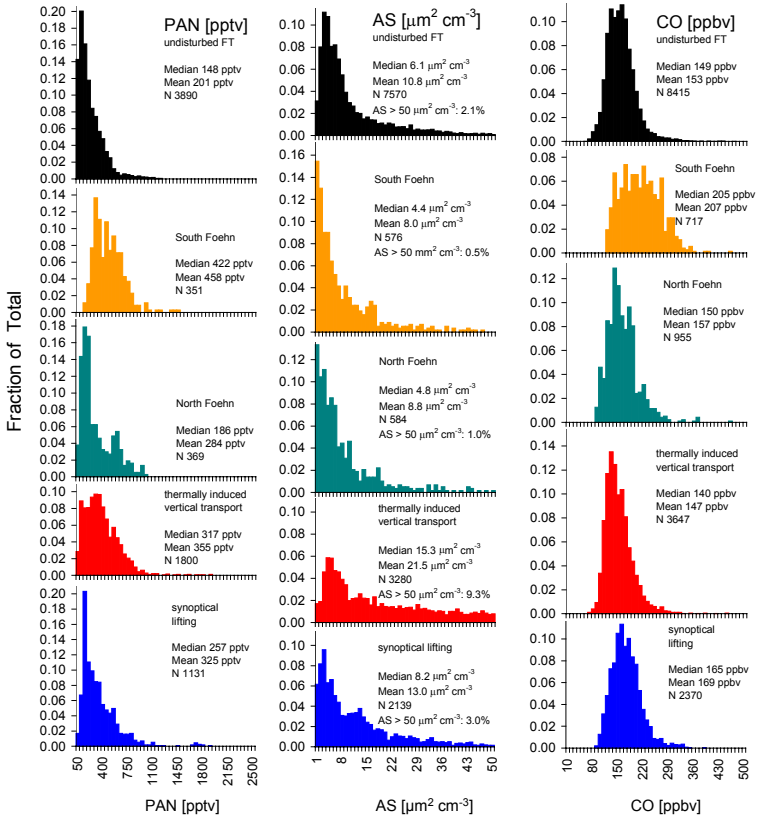

Fig. 5b. Frequency distributions including median, mean and number (*N*) of values for PAN, CO and the aerosol surface area concentration from April 1997 to March 1999 for the whole data set and different meteorological situations. For each species, the data set was based on hourly values and divided into 50 bins.

ACPD
2, 2259–2296, 2002

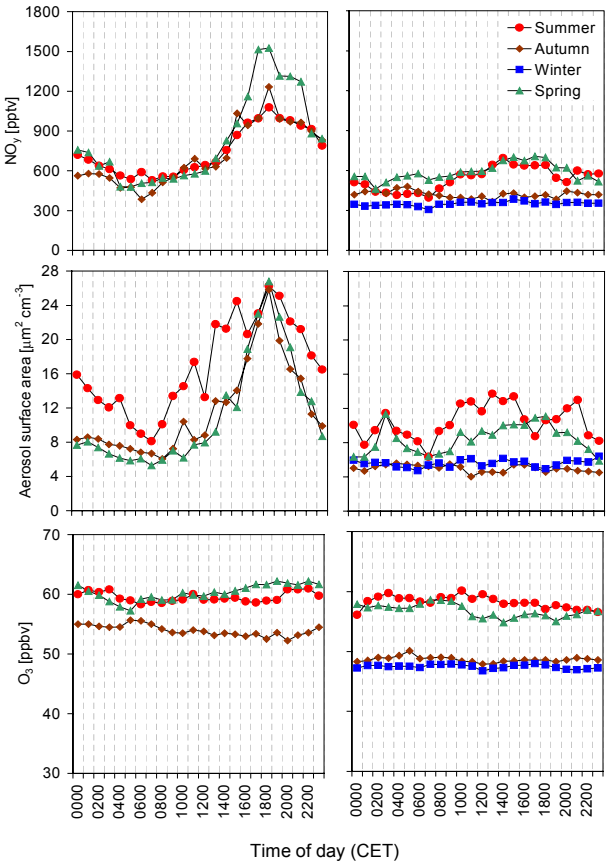

Fig. 6. Diurnal variation of seasonal median values of gas and aerosol parameters from April 1997 to March 1999 at the Jungfraujoch Station. The four seasons are defined as summer, June to August, etc. The left panel shows days with thermally induced vertical transport, whereas undisturbed FT data is shown in the right panel. No winter data are shown for thermally induced vertical transport due to the small number of days with convection during winter.

ACPD
2, 2259–2296, 2002

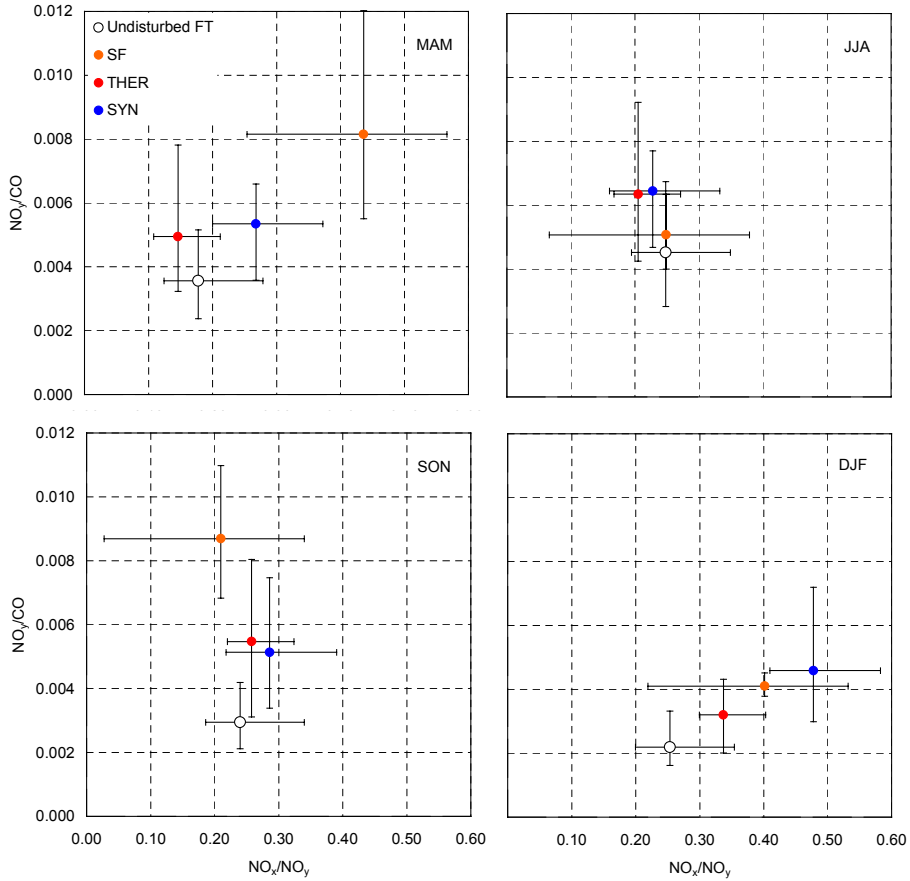

Fig. 7. NO_x/NO_y versus NO_y/CO ratios for south föhn (SF), thermally induced vertical transport (THER), synoptical lifting (SYN) and the undisturbed FT. Four seasons are shown (MAM = March to May, etc.). The first and third quartiles are indicated by bars.

ACPD
2, 2259–2296, 2002

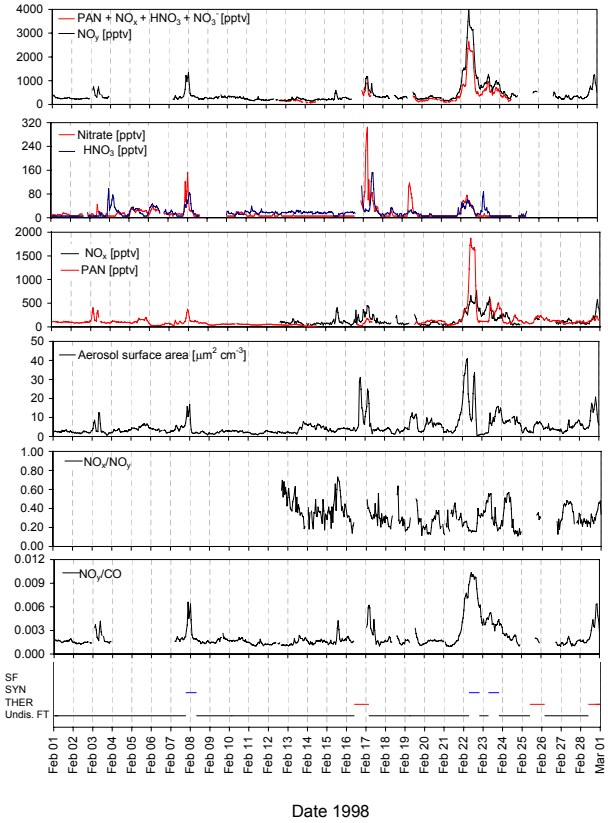

Fig. 8. Time series of hourly mean values of NO_y, HNO_3, NO_3^-, NO_x, PAN, aerosol surface area concentration, the NO_x/NO_y and the NO_y/CO ratios together with the sum of the individually measured NO_y species for February 1998. The occurrence of south föhn (SF), synoptical lifting (SYN), thermally induced vertical transport (THER), and undisturbed FT is also shown.

ACPD
2, 2259–2296, 2002

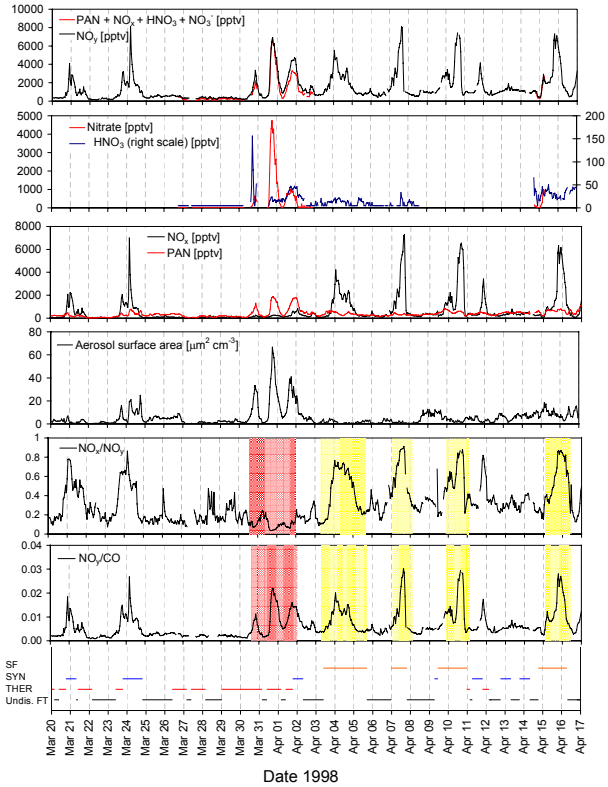

Fig. 9. Time series of hourly mean values of NO_y, HNO_3, NO_3^-, NO_x, PAN, aerosol surface area concentration, the NO_x/NO_y and the NO_y/CO ratios together with the sum of individually measured NO_y species from 20 March to 16 April 1998. The occurrence of south föhn (SF), synoptical lifting (SYN), thermally induced vertical transport (THER), and undisturbed FT is also shown. A period of particular thermally induced vertical transport is highlighted in red, and periods with south föhn events are highlighted in yellow.

ACPD
2, 2259–2296, 2002

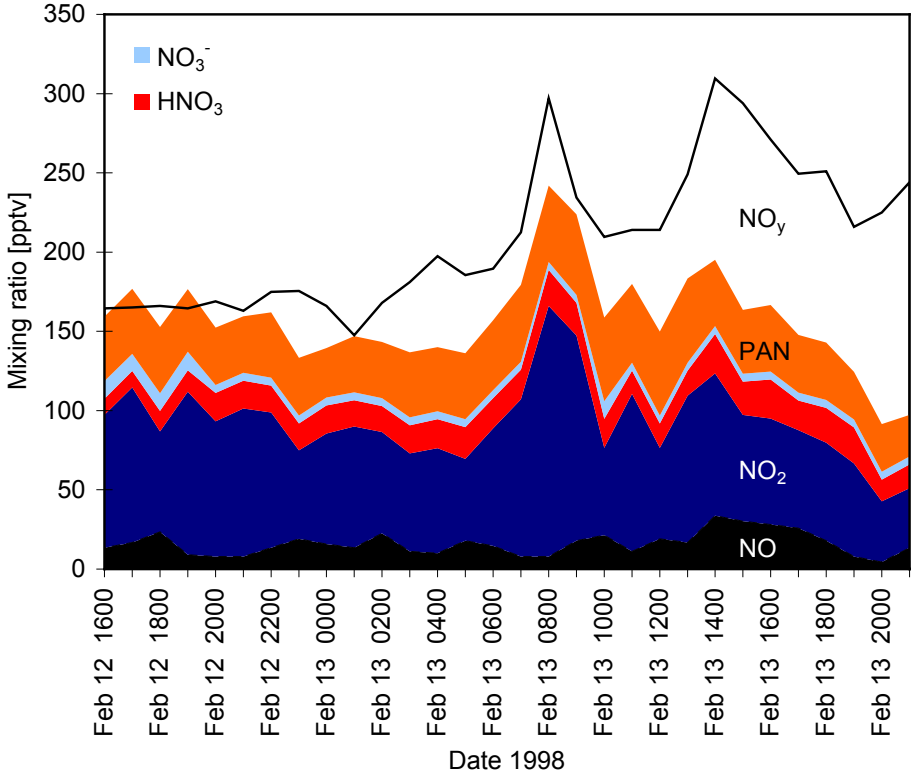

Fig. 10a. Average hourly mixing ratios of speciated and total NO_y at the Jungfraujoch from 12 to 13 February 1998.

ACPD

2, 2259–2296, 2002

Partitioning of NO_y and dependence of meteorological conditions

C. Zellweger et al.

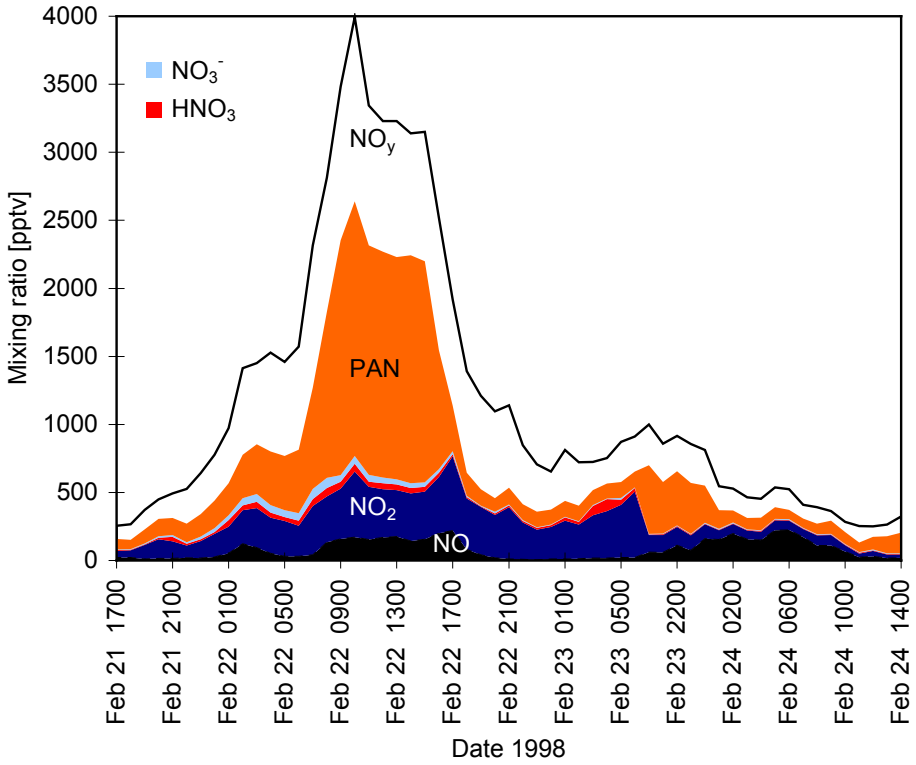

Fig. 10b. Average hourly mixing ratios of speciated and total NO_y at the Jungfraujoch from 21 to 24 February 1998.

ACPD

2, 2259–2296, 2002

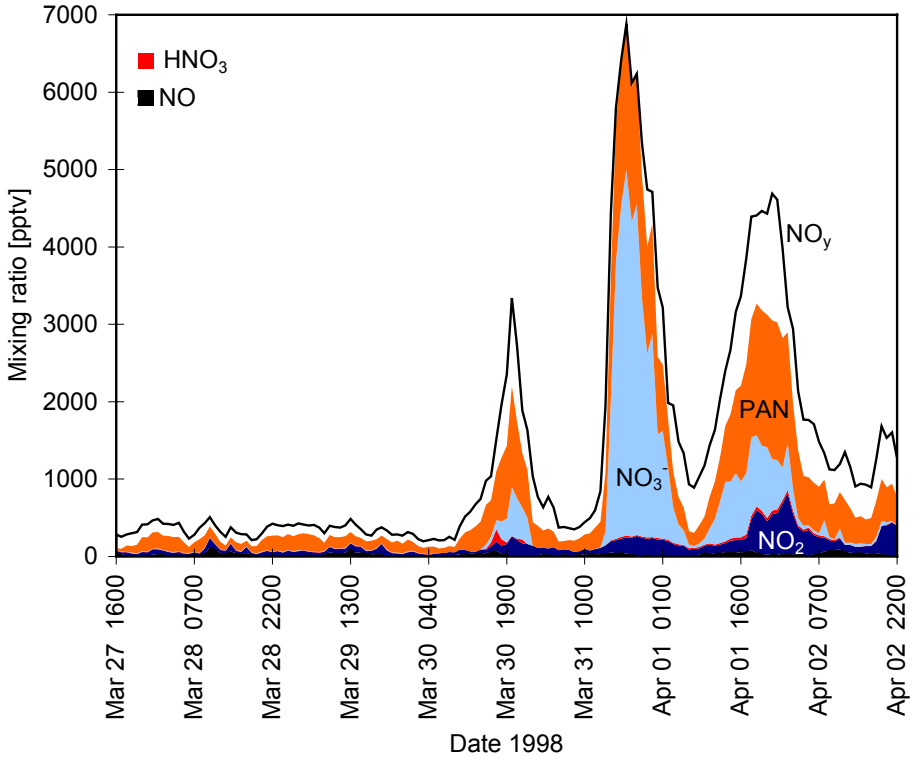

Fig. 10c. Average hourly mixing ratios of speciated and total NO_y at the Jungfraujoch from 27 March to 2 April 1998.

ACPD

2, 2259–2296, 2002

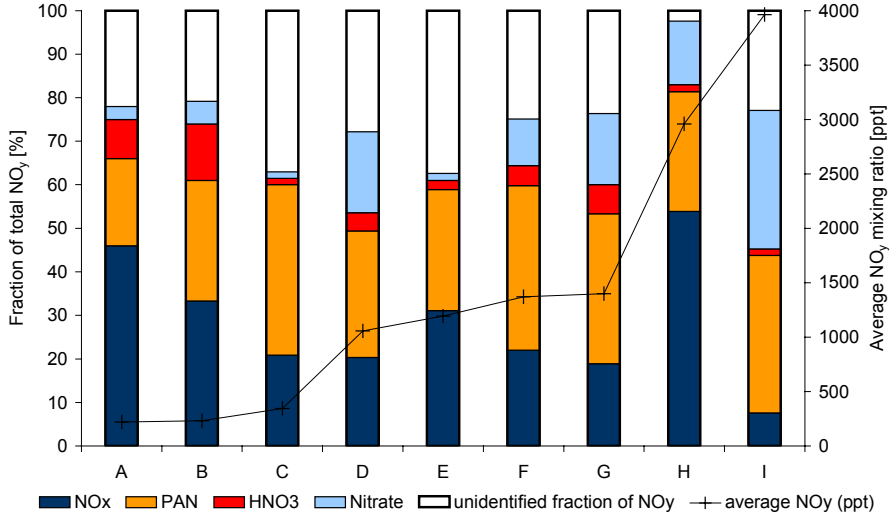

A: winter, undisturbed FT, 12-13 Feb 1998
B: summer, undisturbed FT, 27-30 Jul 1997, 03:00-09:00
C: spring, undisturbed FT, 27-30 Mar 1998
D: summer, influenced by thermally induced vertical transport, 27-30 Jul 1997, 15:00-21:00
E: winter, influenced by synoptical lifting, 22-24 Feb 1998
F: summer, influenced by synoptical lifting, 25 Aug, 19:00 to 26 Aug, 07:00, 1997
G: summer, 16-22 Aug 1997; convective days with low wind speed at the 500 hPa level (Zellweger et al., 2000)
H: spring, south foehn, 14 Apr 1998, 14:00 to 16 Apr 1998, 16:00
I: spring, influenced by thermally induced vertical transport, 30 Mar - 2 Apr 1998, 15:00-21:00

Fig. 11. NO_y levels and speciation for selected periods.